Available online at www.sciencedirect.com
ScienceDirect
Journal of Hazardous Materials 157 (2008) 335–343
Journal of Hazardous Materials
www.elsevier.com/locate/jhazmat

Biodegradation of pyridine by the new bacterial isolates *S. putrefaciens* and *B. sphaericus*

Anil Kumar Mathur [a], C.B. Majumder [b,*], Shamba Chatterjee [c], Partha Roy [c]

[a] *Biotechnology Department, Motilal Nehru National Institute of Technology, Allahabad 211004, India*
[b] *Chemical Engineering Department, Indian Institute of Technology Roorkee, Roorkee 247667, India*
[c] *Biotechnology Department, Indian Institute of Technology Roorkee, Roorkee 247667, India*

Received 8 July 2007; received in revised form 28 December 2007; accepted 31 December 2007
Available online 15 January 2008

Abstract

In this study, two bacterial strains capable of utilizing pyridine as a sole carbon source were isolated from biofilters. Based on the biochemical test, the organisms were identified as *Shewanella putrefaciens* and *Bacillus sphaericus*. In liquid cultures, *S. putrefaciens* and *B. sphaericus* degraded pyridine quite effectively up to 500 mg L^{-1}. *S. putrefaciens* degrades 500 mg L^{-1} of pyridine completely within 140 h, whereas the *B. sphaericus* degrades 500 mg L^{-1} of pyridine only nearly 75% and takes a longer duration of 150 h. *S. putrefaciens* used pyridine as sole carbon and energy source better than *B. sphaericus*. Monod's and Haldane's inhibitory growth models were used to obtain maximum specific growth rate (μ_{max}), half saturation (K_s) and substrate inhibition (K_i) constant for pyridine by using *S. putrefaciens* and *B. sphaericus*. The high value of K_i for *S. putrefaciens* than *B. sphaericus* indicates that the inhibition effect can be observed only in a high concentration range. The *S. putrefaciens* degrades pyridine with a faster rate than *B. sphaericus*. *S. putrefaciens* can be used effectively for the treatment of pyridine bearing wastewater and as an inoculum in a biofilter treating pyridine-laden gas.

Keywords: Pyridine; *Bacillus sphaericus*; *Shewanella putrefaciens*; Growth rate; The half saturation coefficient

1. Introduction

Enormous quantities of aromatic compounds as pollutants are being released into the environment by various industries, because of the broad range of applications of aromatic compounds among the top chemicals used in many industries. Out of this aromatic heterocyclic compounds such as pyridine and its derivatives are of major concern as environmental pollutants due to their recalcitrant, toxic and teratogenic nature. Pyridine is a heterocyclic volatile aromatic compound and is a weak organic base, colorless liquid with penetrating, empyreumatic odor, a threshold odor concentration of 0.1 ppm (58.6 mg L^{-1}) and an odor index of 2390 [1–3]. Pyridine is the parent of a series of chemicals and it is used as a solvent in paint and rubber preparation, as an intermediate in making insecticides and herbicides for agricultural applications and in research laboratories for functions such as extracting plant hormones. It is also used directly in the denaturation of alcohol and to make many different products such as medicines, vitamins, food flavorings, dyes, adhesives and in waterproofing of fabrics [4,5].

Pyridine is classified as a hazardous substance in the USEPA list of priority pollutants [5,6]. It is also mildly toxic for inhalation; its vapor is skin and severe eye irritant and exposure to it can cause depression, gastrointestinal upset, liver and kidney damage, headache, nervousness, dizziness, insomnia, nausea, anorexia, frequent urination, and dermatitis. Exposure to pyridine-laden water or air emissions may have severe health implications [5]. Because of its confirmed carcinogenic properties, the standard set by Occupational Safety and Health Administration (OSHA), American Conference of Governmental Industrial Hygienists (ACGIH) recommended that the exposure limit is 5 ppm average over a 10-h workshift [7]. Thus, researchers have long sought to develop effective, economically feasible techniques for cleaning the atmosphere of waste such as pyridine.

* Corresponding author. Tel.: +91 1332 270492/285059; fax: +91 1332 276535/273560.
E-mail addresses: cbmajumder@yahoo.com, chandfch@iitr.ernet.in (C.B. Majumder).

0304-3894/$ – see front matter © 2008 Elsevier B.V. All rights reserved.
doi:10.1016/j.jhazmat.2007.12.112

Various physico-chemical methods for the treatment of pyridine have been investigated. These include adsorption [3–5,8–10], sorption in zeolites [11], biodegradation [1,2,6,12–18] and ozonation with biodegradation [19]. Among them, biological treatment is an attractive approach for removing pyridine. Pyridine is readily biodegradable and a number of microorganisms degrading pyridine and its derivatives have been a subject of several investigations. Aerobic microorganisms such as *Pseudomonas pseudoalcaligenes-KPN* [1], *Pseudomonas* sp. [2], *Bacillus coagulans* and *Bacillus* sp. [12,13], *Bacillus consortia* [14], *Nocardioides* sp. [15], *Corynebacterium* sp. and *Brevibacterium* sp. [20,21], *Micrococcus* sp. [22], *Nocardia* [23] and *Pimelobacter* [17,24] are known to degrade pyridine. Reports of pyridine treatment in suspended aerobic bioreactor systems for liquid effluent are available [2,6,13,14,25] and only Pandey et al. [1] has reported biotreatment of waste gas containing pyridine using biofilter systems. However, no work has been reported on the biodegradation of pyridine in aqueous medium with *Shewanella putrefaciens* and *Bacillus sphaericus*. Till date several works are in progress to isolate new and efficient microbial species to degrade pyridine. The objective of the present study was to isolate and characterize a bacterial strain capable of degrading high strength of pyridine and to identify the optimum conditions under which this strain can most efficiently breakdown pyridine.

2. Materials and methods

2.1. Chemicals and growth medium

The strain was grown on basal salts medium (BSM) prepared with deionized water (Milli-Q Millipore 18.2 $M\Omega\,cm^{-1}$ resistivity) with pyridine as the sole carbon source. The BSM was sterilized in three parts to avoid precipitation of solution during autoclaving. These were denoted as solutions A, B and C (Table 1). Three stock solutions were prepared and filtered aseptically (0.45 μm filter, Sartorius, Goettingen, Germany) to prevent precipitation during storage. All the chemicals used were AR grade with more than 99% purity and purchased from local chemical manufacturer (S.D. Fine Pvt. Ltd., India, Ranbaxy Laboratories Ltd., India). Other bacteriological grade chemicals were from Himedia (Mumbai, India).

Table 1
Composition of the basal salts medium

Component	Concentration ($g\,L^{-1}$)	Solution
KH_2PO_4	0.91	A
$Na_2HPO_4{\cdot}2H_2O$	2.39	A
KNO_3	2.96	A
$(NH_4)_2SO_4$	1.97	A
$MgSO_4{\cdot}7H_2O$	0.5	B
$CaCl_2{\cdot}2H_2O$	0.5	B
$FeSO_4{\cdot}7H_2O$	0.02	C
$MnSO_4{\cdot}7H_2O$	0.0008	C
$ZnSO_4{\cdot}7H_2O$	0.0004	C
$Na_2MoO_4{\cdot}2H_2O$	0.001	C
$CoCl_2{\cdot}6H_2O$	0.0004	C

2.2. Isolation of strains

Samples were obtained from biofilters I and II, which had been operated for more than one year to remove the mixture of BTEX and MTBX, respectively. Initially compost was used as microbial source in biofilter I and activated sludge was used in biofilter II, respectively. One gram of sample was taken with sterile steel forceps from both the biofilters. The withdrawn samples were mixed with 10 mL of Millipore water and then shaken in a vortex shaker for 10 min and then converted to desire concentration through serial dilution technique. Diluted sample was then allowed to stand for 10 min. One milliliter of this sample was serially diluted up to 10^{-10} in sterile buffer (phosphate buffer, pH 7.0). Serially diluted sample was then spread aseptically on basal salts medium agar 2% (w/v) plates with pyridine as a sole carbon and energy source. The plates were incubated at $30 \pm 1\,^{\circ}C$ and colonies developed were carefully observed for their uniformity and differences. Single colonies were obtained by repeated sub culturing and plating on nutrient agar plate with pyridine, respectively. By this process, one isolate chosen from both biofilters were found to have grown profusely. Maintenance of isolated strain was done by periodical transfer onto nutrient agar slant and was stored at $4\,^{\circ}C$ for further study.

2.3. Strain identification

The morphological, physiological and biochemical tests of two isolates from biofilters I and II are listed in Table 2. These two bacterial strains were taxonomically identified from MTCC, IMTECH, Chandigarh, India, as *B. sphaericus* (Gram-positive) and *S. putrefaciens* (Gram-negative) and were assigned a number MTCC-8103 and 8104, respectively. These two bacterial strains were further confirmed by 16S rDNA sequence analysis.

2.4. Genomic DNA isolation and sequencing of 16S rDNA gene (rDNA)

Genomic DNA was isolated using standard procedures as mentioned in our earlier study [26]. The following primers were used for PCR amplification of the 16S ribosomal DNA: 63f (5′-AGGCCTAACACATGCAAGTC-3′), 1387r (5′-GGGCGGAGTGTACAAGGC-3′) [27]. The PCR mixtures (50 μL) contained 25 pM of each primer, 200 μM of each of deoxynucleoside triphosphate, PCR buffer (Promega, Madison, WI, USA), 0.5 U of Taq DNA polymerase (Promega, Madison, WI, USA) and 10 ng template of DNA. The thermocycling conditions were according to method described earlier [28] consisted of a denaturation step at $94\,^{\circ}C$ for 1 min, 28 amplification cycles of $94\,^{\circ}C$ for 30 s, $55\,^{\circ}C$ for 30 s and $72\,^{\circ}C$ for 1 min and a final polymerization for 4 min with a Thermalcycler (MJ Research, PTC-100, USA). PCR products were visualized on 1.0% agarose gels and the products were excised with Montage DNA gel extraction kit (Millipore Corporation Bedford, MA, USA) following the manufacturer's instructions. The PCR products were cloned in a pGEM-T vector (Promega, Madison, WI, USA) following the manufacturer's instruction. Both strands of the 16S sequences were sequenced by the dideoxynucleotide

Table 2
Biological characteristics of isolated strains

	I	II
Biochemical and culture conditions		
Gram straining	+	−
Klingler iron agar slant	Butt-yellow Slant-red	Butt-red Slant-red
Catalase	+	−
Oxidase	+	+
Indole	−	−
Methyl red	+	−
Voges-Proskauer	+	−
Citrate	−	−
H_2S production	−	+
Glucose	+	−
Maltose	+	−
Sucrose	−	−
Lactose	−	−
Xylose	−	+
Urease	+	+
Ornithine decarboxylase	[a]	+
DNase	[a]	+
L-Arabinose	[a]	+
Morphology under microscope		
Cell type (shape)	Rods	Rods
Color	Yellowish white	Yellowish white
Size	0.5–0.6 × 1.6–2.8 μm	0.5–0.6 × 1.6–2.8 μm
Surface	Smooth	Smooth
Arrangement	Coherent cluster	Isolated
Density	Opaque	Translucent
Elevation	Convex	Convex
Motility	Positive	Positive

[a] Not determined.

method [29]. Nucleotide sequence similarities were determined using BLAST (National Center for Biotechnology Information databases).

2.5. Acclimatization of cultures

B. sphaericus and *S. putrefaciens* were cultivated in 500 mL flask containing 100 mL of the BSM with pyridine as the sole carbon. The cultures were acclimatized to pyridine by exposing the culture in a series of shake flasks. The startup of acclimatization was obtained by inoculating 100 mL of BSM (pyridine concentration, 10 mg L^{-1}) with either *B. sphaericus* or *S. putrefaciens* from nutrient agar slants, under sterile conditions. After forty-eight hours of incubation at 30 °C, 5 mL of this culture was added to fresh BSM (10 mg L^{-1} pyridine) as inoculum. 48 h later, a third fresh BSM was also inoculated with 5 mL of the last culture to ensure that the both bacteria were already adapted to pyridine.

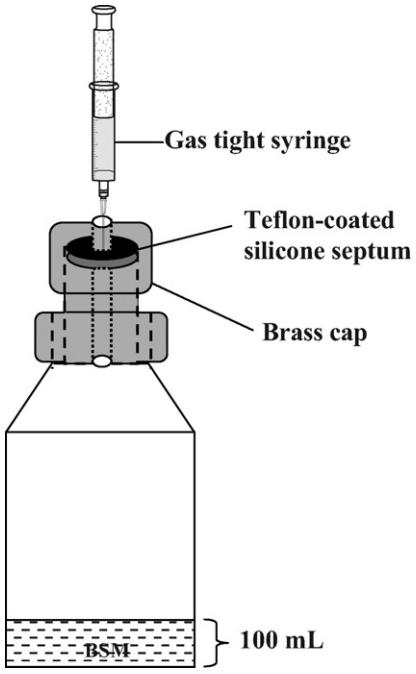

Fig. 1. Schematic diagram of batch experiment.

2.6. Biodegradation kinetics studies

In order to understand the growth pattern of the isolates, the effects of various operating parameters like pH, temperature and growth study was performed in BSM with various concentrations of pyridine. For each batch experiment, one of the following parameters was varied while the others were kept constant: pH, temperature, pyridine concentration, and reaction time (Table 3). Therefore, an experimental program was designed to avoid the possibility of volatilization of pyridine to conduct the batch experiments (Fig. 1). The sampling ports (made of brass) sealed with Teflon-coated silicone septum were provided at the top of bottles to collect liquid samples at regular intervals. During the biodegradation studies experiments were conducted with only 100 mL working volume in a 500 mL of bottles to avoid the deficit of oxygen. Control experiments were also done without microorganisms. Pyridine concentrations in the control bottles (without microorganisms) decreased by 4–5% at the end of each batch study.

In the literature, two approaches are encountered for representing the kinetics of bacterial growth on single substrate.

Table 3
The set of batch experiments of pyridine used to test optimum degradation conditions

Batch test	Parameters varied	Temperature (°C)	pH	Contaminant (mg L^{-1})	Reaction time (h)
1	pH	30	3–11	100	150
2	Temperature	10, 15, 20, 25, 30, 34, 40, 45	7	50, 100	24
3	Reaction time	30	7	100	12, 24,36, 48, 60, 72
4	Contaminate concentration	30	7	50, 100, 200, 500, 1000	150

According to one, substrate is considered non-inhibitory compound and so was represented by Monod's non-inhibitory kinetics equation as given below.

$$\mu = \frac{\mu_{\max} S}{K_S + S} \quad (1)$$

whereas second approach considers the single substrate to be growth inhibitory compound. Haldane inhibitory growth model was selected due to its mathematical simplicity and wide acceptance for representing the growth kinetics of inhibitory substrates. The Haldane's inhibitory growth kinetics equation is as follows:

$$\mu = \frac{\mu_{\max} S}{K_S + S + (S^2/K_i)} \quad (2)$$

In this expression, S is the substrate concentration; μ the specific growth rate; $\mu_{\max}$ the maximum specific growth rate; K_S the half-saturation constant; and K_i is the substrate inhibition constant.

2.7. Analytical methods

Growth of the microorganisms was measured by monitoring the optical density (OD) at 600 nm by using a spectrophotometer (Model Lamda 35, ParkinElmer, USA). The concentrations of pyridine in the aqueous solutions were determined by using a high performance liquid chromatograph (HPLC) (Waters 2487, USA) equipped with a column type Nova pack, C_{18} (3.9 mm × 150 mm) and a dual λ absorbance detector. The Millipore water was used as the mobile phase with a flow rate of 1 mL min^{-1}. The wavelength corresponding to the maximum absorbance (λ_{max}) of pyridine was determined by scanning a standard solution of known concentration at different wavelengths. The λ_{max} value, as determined from this plot, was 256 nm. This wavelength was used to prepare a calibration curve between absorbance and pyridine concentration (given in units of mg L^{-1}) in aqueous solution. The linear region of this curve was further used for the determination of pyridine concentration of the unknown sample. Using a sterilized syringe, 3 mL of aqueous samples were drawn from the shake bottles at regular intervals. A 1 mL sample was then transferred to a gas-tight centrifuge tube (Eppendorf, Germany) and centrifuged (Biofuse Stratos, Germany) at 8000 rpm for 10 min at 4 °C and the supernatant was transferred to a separate eppendorf tubes which were stored at 4 °C before residual pyridine analysis. The remaining 2 mL sample was used for monitoring the optical density in the measurement of the growth of the organisms.

3. Results and discussion

3.1. Extraction of genomic DNA and sequencing of isolated strains

Total genomic DNA was isolated from pure cultures by standard protocol described in Section 2.4. The isolated genomic DNA was stored at −20 °C for further experimental procedure. Afterward, this genomic DNA was used for 16S rDNA analysis.

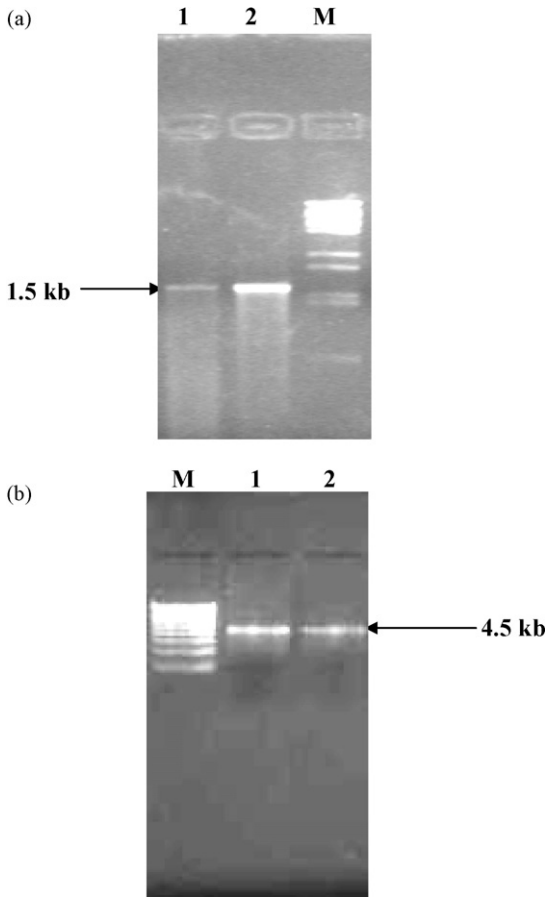

Fig. 2. (a) Lanes 1 and 2 are showing the PCR products (∼1.5 kb) of *B. sphaericus* (AKM 01) and *S. putrefaciens* (AKM 02) with Lambda DNA BstE II digest as marker (M). (b) Lanes 1 and 2 are showing the cloned products (∼4.5 kb) in pGEM-T vector system for *B. sphaericus* (AKM 01) and *S. putrefaciens* (AKM 02), respectively, with 1 kb DNA Ladder as marker (M).

Fig. 2a shows that the corresponding gene fragment was amplified from the genomic DNA, the bands correspond to the anticipated size of ∼1.5 kb. The PCR products generated in this way with Taq polymerase enzyme generally have 'A' overhangs. With the addition of this, these products were ligated in pGEM-T vector using TA cloning method. After ligation reaction the successful clones were selected by Blue-White screening, while colonies having pGEM-T vector with desired insert were selected, and positive clones were isolated. The isolated vector with insert having the desired size of 4.5 kb shown in Fig. 2b. The isolated clones were sequenced from The Centre for Genomic Application (TCGA), New Delhi, India in forward and reverse direction. The sequencing has been done in 3730 Applied Biosystems Genetic Analyzer and analyzed with existing 16S rDNA sequences in the GenBank, EMBL and DDBJ databases. In this way, the taxonomical data were supported and above strains were re-identified as *B. sphaericus* and *S. putrefaciens.*

3.2. Effects of temperature on the biodegradation of pyridine by B. sphaericus and S. putrefaciens

Fig. 3 shows the percentage removal of pyridine by *B. sphaericus* and *S. putrefaciens* for low and high concentration as a

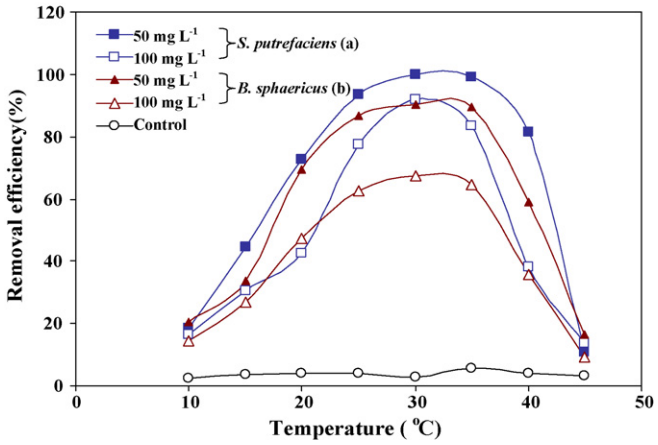

Fig. 3. Effects of temperature on pyridine removal in batch culture by (a) *S. putrefaciens* and (b) *B. sphaericus* at low concentration (50 mg L^{-1}) and high concentration (100 mg L^{-1}) at pH 7.0 for 24 h.

function of temperature at the fixed pH of 7.0 for 24 h. The effects of temperature on the biodegradation of pyridine were observed at low concentration (50 mg L^{-1}) and high concentration (100 mg L^{-1}). The results revealed that the both strains are mesophilic bacteria. It was observed that the percentage removal of pyridine by both organisms increases gradually with the increase in the temperature. Fig. 3 shows an increasing trend in the removal efficiency of pyridine with temperature from 10 to 25 °C, which follows an exponential trend in both the cases (low and high concentrations) for *S. putrefaciens* and *B. sphaericus*. However, between 25 and 35 °C the increase is clearly not exponential. This suggests that the optimum temperature might fall between 25 and 35 °C. Further increase in the temperature (higher than 35 °C) resulted in a remarkable decrease in the removal efficiency of pyridine in both the cases. At the temperatures of 25, 30 and 35 °C, the removal efficiency of pyridine with *S. putrefaciens* was attained as 93.5, 99.8 and 99.3%, respectively, for low concentration and 86.5, 90.5 and 89.4%, respectively, for high concentration. The same trend was also observed in the removal of pyridine with *B. sphaericus* at 25, 30 and 35 °C, but showing lower efficiencies of 86.6, 90.5 and 89.4% for low concentration and 62.6, 67.5 and 64.7 for high concentration were observed, respectively. It is clear from Fig. 3 that the rate of biodegradation of pyridine with *S. putrefaciens* was relatively higher than the *B. sphaericus*, but was reduced significantly in both the cases at above 35 °C. The results reveal that *B. sphaericus* and *S. putrefaciens* can grow from 10 to 35 °C but the maximum removal is at the temperature of 30 °C.

3.3. Effects of pH on the biodegradation of pyridine

pH has a significant effect on the degradation efficiency of the strains. The removal of pyridine of 100 mg L^{-1} by *B. sphaericus* and *S. putrefaciens* at various initial pH values are shown in Fig. 4a and b. *S. putrefaciens* removed the pyridine completely within 110, 56, 36, 60 and 77 h, respectively, when the initial pH values were 5, 6, 7, 8 and 9. For *B. sphaericus*, pyridine was removed completely within 120, 72, 51, 80 and 120 h, respectively, when the initial pH values were 5, 6, 7, 8 and 9. Fig. 4a and b show that the degradation time of pyridine of 100 mg L^{-1} concentration with *S. putrefaciens* and *B. sphaericus* at 30 °C and pH 7 were significantly different, i.e. 36 and 51 h, respectively. In comparison to *S. putrefaciens*, *B. sphaericus* took more time for the degradation of pyridine at the same conditions. The percentage removal of pyridine reached maximum at pH 7.0 specifically between the optimum pH of 6.0 and 8.0. Degradation is comparatively less at the outside of the optimum range. This was attributed mainly to the inhibitory effect of superacidity or superalkalinity on the activity of intracellular enzyme of bacteria. The results are consistent with the three reported *S. putrefaciens* strains (MR-4, CN32 and BrY), presenting various and well-characterized over a wide range of pH and ionic strength conditions [30].

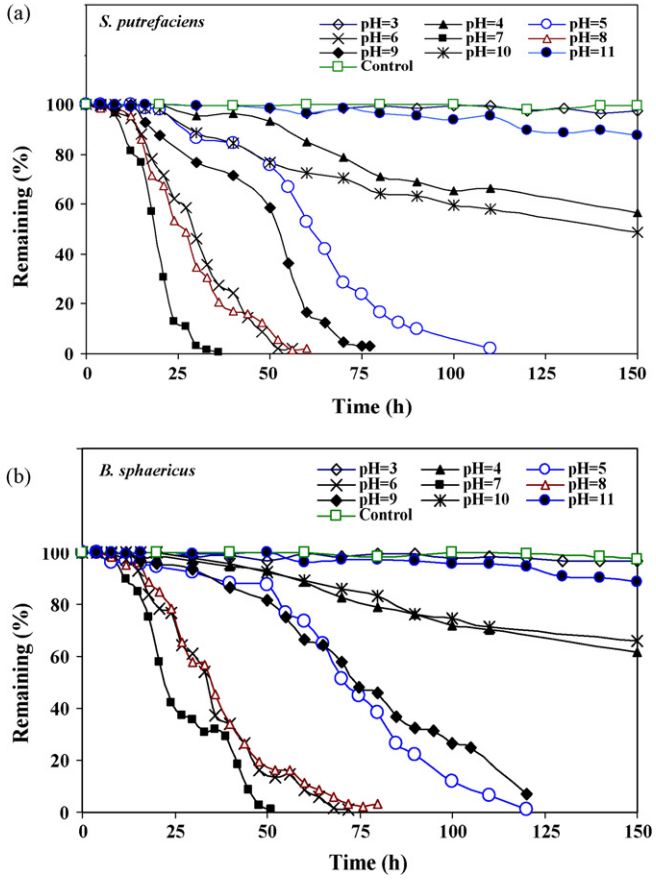

Fig. 4. Effects of pH on pyridine removal in batch culture by (a) *S. putrefaciens* and (b) *B. sphaericus*.

3.4. Pyridine biodegradation by S. putrefaciens and B. sphaericus in batch culture

The results of batch studies for pyridine degradation in basal salts medium by *S. putrefaciens* and *B. sphaericus* are given in Fig. 5a and b, respectively. The *S. putrefaciens* degrades about 100, 99.9, 99.9, 98.98 and 22.68% of pyridine with an initial concentration of 50, 100, 200, 500 and 1000 mg L^{-1} in 36, 44, 60, 140 and 150 h, respectively. The *B. sphaericus* degrades

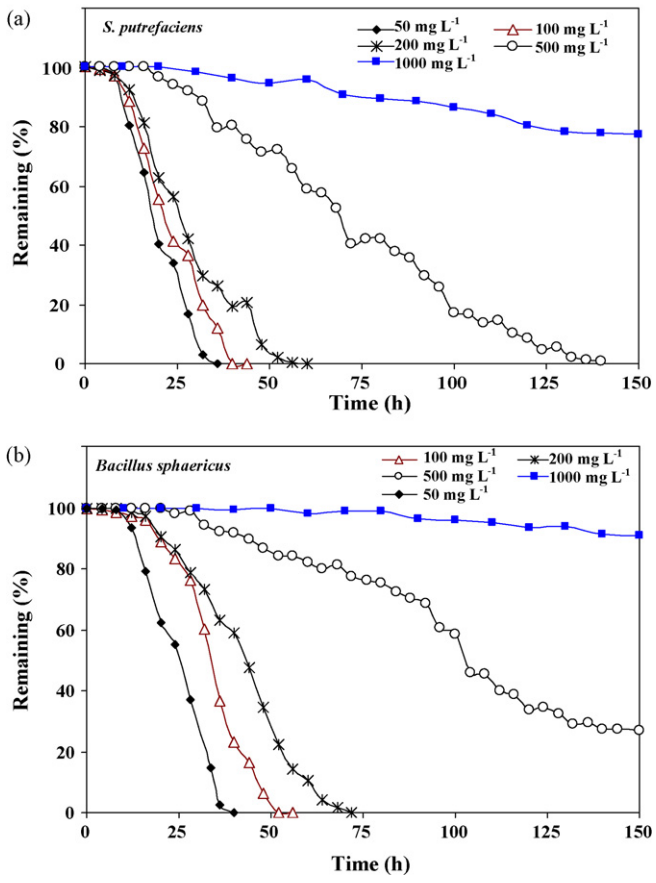

Fig. 5. Degradation of pyridine by (a) *S. putrefaciens* and (b) *B. sphaericus* in batch culture (temperature = 30 ± 0.2 °C, pH 7.0).

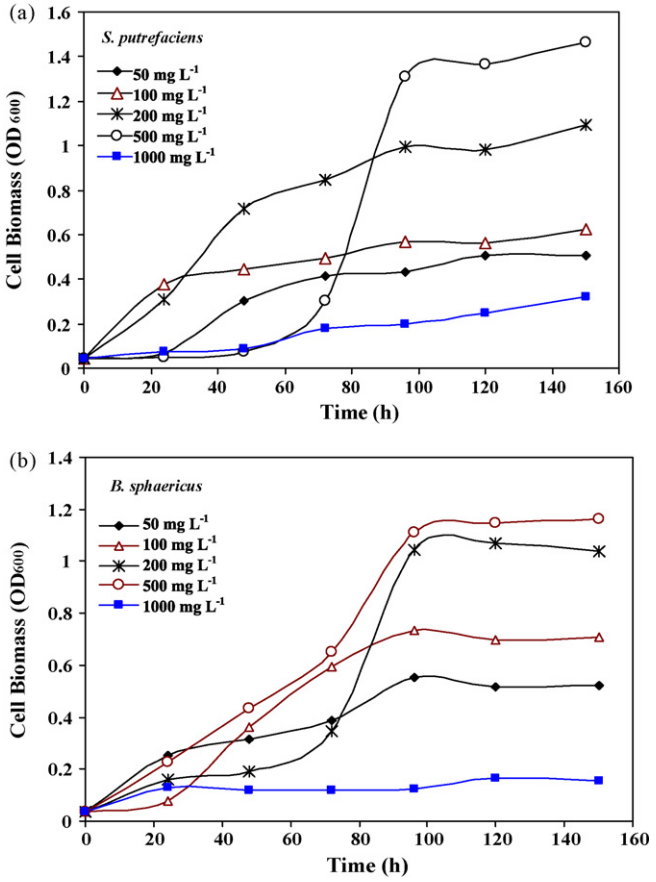

Fig. 6. Growth of (a) *S. putrefaciens* and (b) *B. sphaericus* in pyridine (temperature = 30 ± 0.2 °C, pH 7.0).

about 100, 99.8, 99.9, 72.3 and 8.9% of pyridine with an initial concentration of 50, 100, 200, 500 and 1000 mg L^{-1} in 40, 52, 72, 150 and 150 h, respectively. At high concentrations, it was observed that towards the end of the substrate consumption curve, there is a region of relatively reduced rate of substrate removal. Results show that the degradation time of pyridine was low at low substrate concentration since degradation rate is high at low substrate concentration. It also shows that at the higher concentration of pyridine degradation rate is low and degradation time is high. Three possible explanations may be offered at this stage, firstly, the deficit of oxygen, since these experiments were done in bottles of 500 mL with 100 mL working volume. These experiments performed in bottle, clearly showed that the culture was not able to degrade efficiently the high concentration of pyridine under the hypoxic conditions in bottles. Morgan et al. [31] has also reported that oxygen supply was the factor limiting BTEX biodegradation in ground water environments. Secondly, an exponential phase, a drop in oxygen concentration may be a possible reason for low growth rate [32]. Thirdly, the slight (<10%) fall in pH of the solution over time may be another reason, since pyridine is a heterocyclic aromatic compound and is a weak organic base. Low values of both oxygen and pH may affect the kinetics of substrate consumption adversely [33]. Out of the two isolates, rate of pyridine biodegradation was more by *S. putrefaciens* than that of *B. sphaericus*.

3.5. Growth of *S. putrefaciens* and *B. sphaericus* in pyridine

The growth of both organisms increased with the increase in pyridine concentration (Fig. 6a and b). But the lag phase was extended at higher concentrations of pyridine, which demonstrated positive correlation between cell biomass and pyridine degradation. In the batch studies, the biomass concentrations of *S. putrefaciens* and *B. sphaericus* were initially low, but later on growth increases exponentially. The results showed that in the lag period, the biodegradation time and the maximum microorganism concentration increased on increasing the substrate concentrations. Biodegradation rates were calculated as total degradation of substrate concentration per total degradation time and cell concentration obtained. It is clear from these figures (Fig. 6a and b) that the pyridine was utilized by *S. putrefaciens* and *B. sphaericus* effectively up to 500 mg L^{-1}. But the *S. putrefaciens* used pyridine as sole carbon and energy source better than *B. sphaericus*. The previous reports mainly on biodegradation of pyridine in batch process were in the range of 50–300 mg L^{-1} by using *P. pseudoalcaligenes-KPN* [6] and at pyridine concentration of 750 mg L^{-1} by using *Pseusdomonas* (P12) where the maximum 90% degradation was achieved after 8 days of shaking period [2]. In continuous process, the degradation of pyridine by using *P. pseudoalcaligenes-KPN* in aqueous phase was more than 97.6% at a loading rate of 0.251 kg pyridine kg MLSS^{-1} day^{-1} (influent concentration 300 mg L^{-1} pyri-

Table 4
Growth kinetics parameter values of Monod's model and Haldane's model for biodegradtion of pyridine using *S. putrefaciens* and *B. sphaericus*

Microorganism	Monod's model		Haldane's model			Errors[a]	
	μ_{max} (h^{-1})	K_s (mg L^{-1})	μ_{max} (h^{-1})	K_s (mg L^{-1})	K_i (mg L^{-1})	STDEV	R^2
S. putrefaciens	0.033	90.74	0.0424	122.74	616.3736	0.00449	0.667
B. sphaericus	0.041	146.28	0.0481	134.28	418.685	0.00018	0.896

[a] Only applicable for Haldane's model.

dine) [6] and in gaseous phase more than 99% of pyridine was removed from contaminated gas at a below loading less than of 434 g pyridine m^{-3} h^{-1} by using mixture of compost, wood chips and *P. pseudoalcaligenes-KPN* as a packing materials in biofilter [1].

3.6. Growth kinetics

The specific growth rates (μ) of *S. putrefaciens* and *B. sphaericus* and initial concentration of pyridine have been plotted in Fig. 7. Here, specific growth rate increases initially with the increase in initial pyridine concentration up to a certain concentration level for both bacteria, then it starts decreasing with the increase in the pyridine concentration. Kinetic constants were estimated by specific growth rate data from low concentration region and were fitted to Monod's model (Fig. 7). It has been found that Monod's model cannot represent the data over entire concentration range. Haldane inhibitory growth model can represent the data of entire region in Fig. 8a and b for *S. putrefaciens* and *B. sphaericus*, respectively. The values of the growth kinetics of pyridine estimated by Monod's and Haldane model for *S. putrefaciens* and *B. sphaericus* are presented in Table 4. The maximum specific growth rate (μ_{max}), half saturation (K_s) and substrate inhibition (K_i) constant and values of pyridine in Table 4 for both the microorganisms are of quite significance than the values reported in the literature for pyridine [6]. Kotturi et al. [34] noted that the K_s value is influential on the growth kinetics in low concentration region. At the same time, the small changes in the biomass and substrate concentrations in batch reactors cannot be measured accurately. Therefore, this

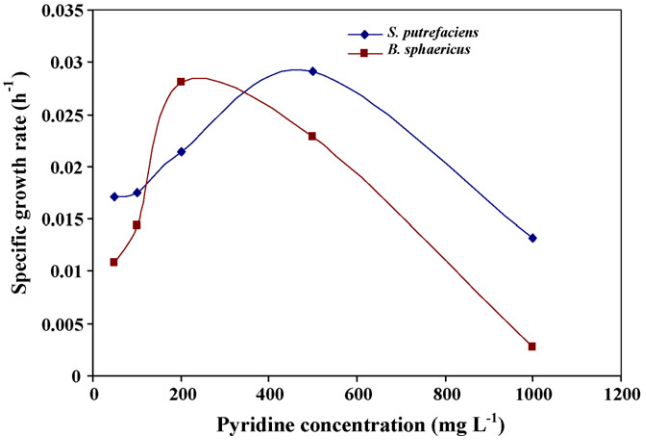

Fig. 7. Effect of pyridine on specific growth rate of *S. putrefaciens* and *B. sphaericus*.

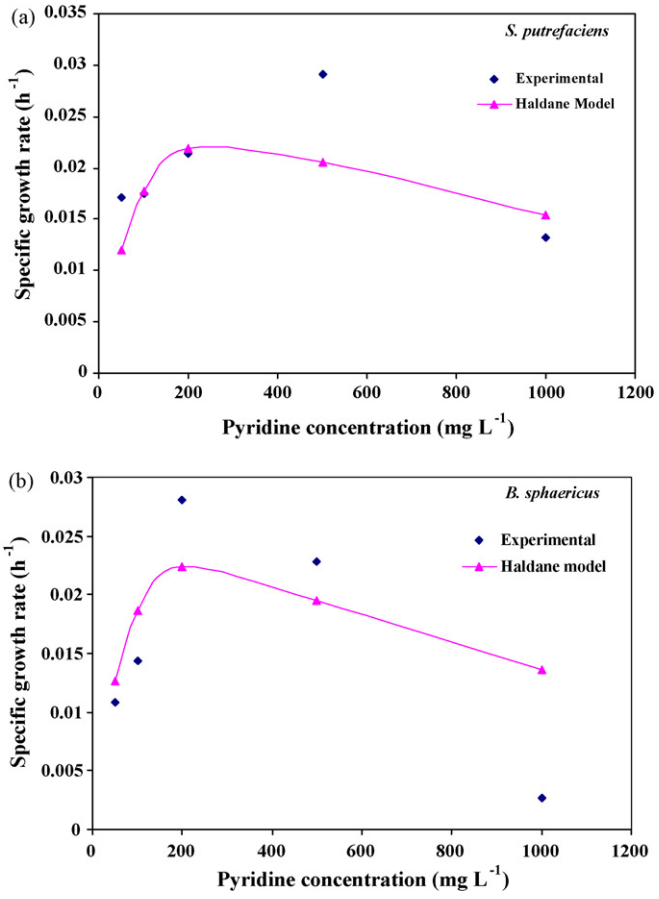

Fig. 8. Haldane's growth model fitted to results of batch growth experimental data to determine biokinetics parameters (a) *S. putrefaciens* and (b) *B. sphaericus*.

may be one possible reason for the discrepancy in the values of K_s for *S. putrefaciens* and *B. sphaericus*. In the literature, there are no data for K_i value of pyridine. The high value of K_i for *S. putrefaciens* than *B. sphaericus* indicates that the inhibition effect can be observed only in a high concentration range. Fig. 8a shows that the model data are more deviating than the experimental data of *S. putrefaciens* with more standard deviation of error (STDEV) and correlation coefficient (R^2) as compared to *B. sphaericus* (Fig. 8b and Table 4). This more deviation may be due to the characteristics of bacteria and the experimental error induced in the estimation of the kinetic model parameters.

4. Conclusion

The purposes of this study were to isolate the pyridine degrading bacteria from the biofilters and to investigate its

physiological characteristics. The two pure stains were isolated and identified as *S. putrefaciens* and *B. sphaericus*. This experimental results show that among the isolated stains, *S. putrefaciens* degrades 500 mg L^{-1} of pyridine completely within 140 h, whereas the *B. sphaericus* degrades 500 mg L^{-1} of pyridine only nearly 75% after 150 h, implying *S. putrefaciens* used pyridine as sole carbon and energy source better than *B. sphaericus*. The maximum growth rate and the half saturation coefficient of *S. putrefaciens* were 0.033 h^{-1} and 90.74 mg L^{-1}, respectively. For *B. sphaericus*, the maximum growth rate and the half saturation coefficient was 0.041 h^{-1} and 146.28 mg L^{-1}, respectively. The strain *B. sphaericus* takes more time and is less efficient for the degradation of pyridine above or equal to 500 mg L^{-1} in comparison to *S. putrefaciens*. Isolate *S. putrefaciens* can degrade high strength pyridine and compared to the other organisms reported in the literature, the strain *S. putrefaciens* was capable of degrading 500 mg L^{-1} of pyridine effectively. Monod's and Haldane's inhibitory growth model were used to obtained maximum growth rate, half saturation and substrate inhibition constant for pyridine by using *S. putrefaciens* and *B. sphaericus*. Monod's model could not represent the growth kinetics over the studied concentration range. However, Haldane's inhibitory growth kinetics model could be fitted to the growth kinetics data well for entire range of concentration. The high value of K_i for *S. putrefaciens* than *B. sphaericus* indicates that the inhibition effect can be observed only in a high concentration range. At this point the information presented herein lay the foundation for further treatment of pyridine bearing wastewater and the use of an inoculum of *S. putrefaciens* in a biofilter treating pyridine-laden gas.

Acknowledgements

The authors express their gratitude to the reviewers for their useful comments. Authors are very thankful to the Ministry of Human Resource and Development (MHRD), Government of India for providing financial support to undertake the work.

References

[1] R.A. Pandey, K.V. Padoley, S.S. Mukherji, S.N. Mudliar, A.N. Vaidya, A.S. Rajvaidya, T.V. Subbarao, Biotreatment of waste gas containing pyridine in a biofilter, Bioresour. Technol. 98 (2006) 2258–2267.

[2] S.V. Mohan, S. Sistla, R.K. Guru, K.K. Prasad, C.S. Kumar, S.V. Ramakrishna, P.N. Sarma, Microbial degradation of pyridine using *Pseudomonas* sp. and isolation of plasmid responsible for degradation, Waste Manag. 23 (2003) 167–171.

[3] D. Mohan, K.P. Sing, S. Sinha, D. Gosh, Removal of pyridine from aqueous solution using low cost activated carbons derived from agricultural waste materials, Carbon 42 (2004) 2409–2421.

[4] D. Mohan, K.P. Sing, S. Sinha, D. Gosh, Removal of pyridine derivatives from aqueous solution by activated carbons developed from agricultural waste materials, Carbon 43 (2005) 1680–1693.

[5] D.H. Lataye, I.M. Mishra, I.D. Mall, Removal of pyridine from aqueous solution by adsorption on bagasse fly ash, Ind. Eng. Chem. Res. 45 (2006) 3934–3943.

[6] K.V. Padoley, A.S. Rajvaidya, T.V. Subbarao, R.A. Pandey, Biodegradation of pyridine in a completely mixed activated sludge process, Bioresour. Technol. 97 (2006) 1225–1236.

[7] Agency for Toxic Substances and Disease Registry U.S. Public Health Service, Toxicological Profile for Pyridine, 1992, pp. 61–62.

[8] R. Kumar, I.M. Mishra, I.D. Mall, Treatment of pyridine bearing wastewater using activated carbon, Res. Ind. 40 (1995) 33.

[9] S. Zhu, P.R.F. Bell, P.F. Greenfield, Adsorption of pyridine onto spent Rundle oil shale in dilute aqueous solution, Water Res. 22 (10) (1988) 1331–1337.

[10] E. Sabah, M.S. Celik, Interaction of pyridine derivatives with sepiolite, J. Colloid Interface Sci. 251 (2002) 33.

[11] H. Bludau, H.G. Karge, W. Niessen, Sorption, sorption kinetics and diffusion of pyridine in zeolites, Micropor. Mesopor. Mater. 22 (1998) 297.

[12] B. Uma, S. Sandhya, Pyridine degradation and heterocyclic nitrification by *Bacillus coagulans*, Can. J. Microbiol. 43 (1997) 595–598.

[13] B. Uma, S. Sandhya, Kinetics of pyridine degradation along with toluene and methylene chloride with *Bacillus* sp., Bioproc. Eng. 18 (1998) 303–305.

[14] T.S. Uma, S. Sandhya, S. Sathyanarayana, S.N. Kaul, Biodegradation of pyridine from pharmaceutical wastewater using *Bacillus consortia*, J. IAEM 29 (2002) 76–80.

[15] S.K. Rhee, K.Y. Lee, J.C. Chung, S.T. Lee, Degradation of pyridine of *Nocardioides* sp. strain OS4 isolated from the toxic zone of a spent shale column, Can. J. Microbiol. 43 (1997) 205–209.

[16] Y. Li, G. Gu, J. Zhao, H. Yu, Anoxic degradation of nitrogenous heterocyclic compounds by acclimated activated sludge, Process Biochem. 37 (2001) 81–86.

[17] S.K. Rhee, G.M. Lee, S.T. Lee, Influence of a supplementary carbon source on biodegradation of pyridine by freely suspended and immobilized *Pimelobacter* sp., Appl. Microbiol. Biotechnol. 44 (1996) 816–822.

[18] S. Fetzner, Bacterial degradation of pyridine, indole, quinoline, and their derivatives under different redox conditions, Appl. Microbiol. Biotechnol. 49 (1998) 237–250.

[19] M. Stern, H. Elmar, O.M. Kut, K. Hungerbouhler, Removal of substituted pyridines by combined ozonation/fluidized bed biofilm treatment, Water Sci. Technol. 35 (1997) 329–335.

[20] O.P. Shukla, S.M. Kaul, A constitutive pyridine degrading system in *Corynebacterium* sp., Indian J. Biochem. Biophys. 11 (1974) 201–207.

[21] O.P. Shukla, S.M. Kaul, Succinate semialdehyde an intermediate in the degradation of pyridine by *Brevibacterium* sp., Indian J. Biochem. Biophys. 12 (1975) 321–330.

[22] G.K. Sims, L.E. Sommers, A. Konopka, Degradation of pyridine by *Micrococcus luteus* isolated from soil, Appl. Environ. Microbial. 51 (1986) 963–968.

[23] R.A. Panday, S. Sandhya, Degradation of heterocyclic bases by mixed *Nocordia* sp. isolated from soil, J. Environ. Sci. Health A Environ. Sci. Eng. 26 (1991) 1081–1103.

[24] S.K. Rhee, G.M. Lee, S.T. Lee, Influence of A supplementary carbon source on biodegradation of pyridine by freely suspended and immobilized *Pimelobacter* sp., Appl. Microbiol. Biotechnol. 44 (1996) 816–822.

[25] R.A. Pandey, S. Sandhya, Microbial degradation of heterocylic bases in a completely mixed activated sludge process, J. Environ. Sci. Health A 32 (1997) 1325–1338.

[26] A.K. Mathur, C.B. Majumder, S. Chatterjee, Combined removal of BTEX in air stream by using mixture of sugar cane bagasse, compost and GAC as biofilter media, J. Hazard. Mater. 148 (2007) 64–74.

[27] J.R. Marchesi, T. Sato, A.J. Weightman, T.A. Martin, J.C. Fry, S.J. Hiom, W.G. Wade, Design and evaluation of useful bacterium-specific PCR primers that amplify genes coding for bacterial 16S rRNA, Appl. Environ. Microbiol. 64 (1998) 795–799.

[28] K.S. Na, A. Kuroda, N. Takiguchi, T. Ikeda, H. Ohtake, L. Kato, Isolation and characterization of benzene-tolerant *Rhodococcus opacus* stratins, J. Biosci. Bioeng. 4 (2005) 378–382.

[29] F. Sanger, S. Nicklen, A.R. Coulson, DNA sequencing with chain-terminating inhibitors, Proc. Natl. Acad. Sci. U.S.A. 74 (1977) 5463–5467.

[30] E. Dague, J.D.F. Jorand, F. Thomas, F. Gaboriaud, Probing surface structures of *Shewanella* sp. by microelectrophoresis, Biophys. J. 90 (2006) 2612–2621.

[31] P. Morgan, S.T. Lewis, R.J. Watkinson, Biodegradation of benzene, toluene, ethylbenzene and xylenes in gas-condensate-contaminated ground-water, Environ. Pollut. 82 (1993) 181–190.
[32] R.D. Yang, A.E. Humphrey, Dynamic and steady state studies of phenol biodegradation in pure and mixed cultures, Biotechnol. Bioeng. 17 (1975) 1211–1235.
[33] H.W. Blanch, D.S. Clark, Biochem. Eng., Marcel Dekker Inc., New York, 1996.
[34] G. Kotturi, C.W. Robinson, W.E. Inniss, Phenol degradation by a psychrotropic strain of *Pseudomonas putida*, Appl. Microbiol. Biotechnol. 34 (1991) 1217–1223.